

# Nigerian Journal of Physics (NJP)

ISSN online: 3027-0936 ISSN print: 1595-0611

DOI: https://doi.org/10.62292/njp.v34i3.2025.438

Volume 34(3), September 2025



# The Effect of the Film-to-Focus Distance (FFD) Method on the Optical Density of the Organs and Anatomical Interest Parts in the Thoracic Cage

\*1Nabasu, S. E., 2Songden, S. D., 1Kyense, D. K., 3Sirisena, U. A. I., 1Joseph, D. Z., 1Joseph, P. B., 3Dembo, J. S., 1Weng, Y. C., 1Dang, D. Y. and 1Freeman, N.

<sup>1</sup>Department of Physics, Plateau State University, Bokkos, Plateau State, Nigeria.

<sup>2</sup>Department of Physics, University of Jos, Plateau State, Nigeria.

<sup>3</sup>Department of Radiology, Medical Physics Unit, Jos University Teaching Hospital, Jos, Nigeria.

\*Corresponding Author's Email: <a href="mailto:nabasuseth882@gmail.com">nabasuseth882@gmail.com</a>

#### **ABSTRACT**

The effect of the Film-Focal Distance (FFD) technique on the optical density of the parts of anatomical interest and the organs within the thoracic cage was determined to identify a quality radiograph that is required by the Radiologists to accurately interpret and conclude the diagnosis from Chest X-ray (CXR) films. A PHILIPS MCD-105 mobile portable X-ray machine with a maximum voltage of 105 kVp was used in this study. AGFA X-ray films were used to obtain all the chest radiographs. A perspex phantom was constructed to house the rib cage of a human adult obtained from the anatomy laboratory. The whole phantom arrangement was to simulate the chest part of an adult human. The phantom was exposed five times, maintaining a constant voltage of 70 kV and a tube load of 10 mAs, by varying the FFDs at 110, 120, 130, 140, and 150 cm. A RaySafe Thin-X RAD dosemeter was used to determine the doses delivered to the Phantom. An X-Rite 331 transmission densitometer was used to determine the optical densities of the required areas. It was noted that both the FFDs and optical densities of the recorded areas have an inverse relationship, confirming that FFD has a significant effect on the quality of any X-ray film in chest X-ray examinations. Even though the radiograph at FFD 150 cm had the best contrast of them all due to low exposure, the radiograph at FFD 140 cm was found to give the optimum image quality of the parts of anatomical interest and the positions of the organs enclosed in the rib cage, with a dose even lower than the internationally accepted maximum value.

## **Keywords:**

Optical density, Film-Focal Distance (FFD), Chest X-Ray (CXR), Thoracic cage, RaySafe Thin-X RAD, Dosemeter.

#### INTRODUCTION

Recent studies indicate both radiologists and patients are becoming increasingly concerned about the excessively high radiation levels being administered during normal X-ray exams. This implies that after a justified assessment, the imaging technique needs to be enhanced by making sure the radiation dosage is as low as reasonably attainable (ALARA) and compatible with an image of excellent diagnostic quality. Nonetheless, doing so would achieve the therapeutic objective of the evaluation with the least degree of patient risk (Brennan et al., 2004)(Seth et al., 2022). As digital systems advance, it may be possible to reduce radiation exposure while improving image quality; still, this will require adjusting technological aspects to produce high-quality X-ray images. According to the "as low as reasonably

achievable" (ALARA) principle, the challenge is to identify the right settings to minimize the patient's effective dose while still providing a high-quality image to provide the best possible diagnosis (Vano et al., 2007)(Peters & Brennan, 2002).

The risks of ionising radiation have long been known, as have the levels and hazards connected to high doses (trial use and nuclear explosions). In diagnostic radiology, the risks from the far lower levels have been harder to evaluate. The adoption of all known techniques to reduce the dose as much as possible without compromising the quality of the radiographs is necessary because there is no safe exposure level beyond which harmful effects stop occurring (Seth et al., 2022).

Radiographic density or optical density is reflected by radiographic image darkness. It is known as "transmitted density" in traditional film radiography, as it measures the light transmitted through the film. It refers to how far the image's overall histogram is moved towards the lower grey levels in digital imaging (White & Pharoah, 2013). Some factors that affect the radiographic or optical density of conventional film and digital receptor or plate are changes in mA and in exposure time, changes in kVp, changes in source-to-object distance and thickness of the absorber (Bushberg & Boone, 2011)(Bushberg et al., 1994)(Curry et al., 1990)(Miles, 2009)(Walter, 2010). Many Radiology departments perform chest X-ray (CXR) examinations regularly to diagnose diseases and injuries (Veldkamp et al., 2009)(Venema et al., 2005). Chest Radiography, although one of the most important procedures for detecting various illnesses, accounts for 30 to 40% of all radiographs performed. As a result, improving image quality and reducing radiation dosage are major study areas (Valentin, 2004)(Schaefer-Prokop et al., 2008)(Daffner & Hartman, 2013).

Chest X-ray (CXR) has become an important aspect of routine medical examination in many nations throughout the world, whether for admitting students to higher education institutions, staff appointments, or regular medical checkups of individuals for health fitness(Idris & Abdul Manaf, 2012). In the detection of neonatal lung disorders such as rib cage pain (rib cage fracture), Acute heart failure, Pneumonia, and COVID-19 virus, chest X-ray (CXR) has recently been seen as a significant imaging modality alongside lung ultrasound (Liu et al., 2021)(Khan et al., 2012)(Nakao et al., 2021)(Jain et al., 2020)(Mousavi et al., 2022)

This research work prioritised the diagnosis of cases that concern organs enclosed in the thoracic cage and the parts of anatomical interest due to their significance in the human body. To provide a quality chest X-ray film to help physicians in the diagnosis of the diseases of those organs through finding a radiograph of the FFD that will give the optimum image quality in terms of the radiographic density of those organs within the thoracic cage and the parts of anatomical interest with a minimum dose. The work was done in the Radiology department of

Skane Radio Diagnostic Centre/Hospital Nig. Ltd., Jos, Plateau State, Nigeria, contributing to the health of all patients coming to the department for chest X-ray examination and helping globally, especially those using their type of X-ray machine

# MATERIALS AND METHODS Preparation of the Phantom

A rectangular Perspex phantom was constructed with dimensions 29 cm x 20 cm x 56 cm in length, width, and height, respectively. The whole arrangements were made to simulate the chest part of an adult human. The ribcage was fixed in position in the phantom and made stable to avoid floating because the phantom was filled with water to cover the bones completely, which simulates human tissue. The specimen (rib cage) used was an adult human rib cage that was carefully selected from the Anatomy Department, Faculty of Medicine, University of Jos, Plateau State, Nigeria. It was selected out of the specimens used in teaching Medical Students. An MCD-105 Model mobile portable X-ray machine with the highest kVp of 105 kVp was used in irradiating the phantom. The machine is from the Radiology Department of Skane Radiodiagnostic Centre/Hospital, Jos, Plateau State, Nigeria. The manufacturer of the machine is Philips Manufacturing Company, Japan. The machine number is 8814771. The films were AGFA films manufactured by a Belgian company, having dimensions of 14x14 cm and 17x14 cm. The exposed films were manually processed and dried using natural sunlight. A RaySafe ThinX dosemeter was used to measure the doses. It is an easy tool for fast results and has been optimised to meet the need for a basic multi-parameter instrument for simultaneous measurement of dose, dose rate, kVp, HVL, exposure time and pulses. All parameters were conveniently displayed on the large LCD.

Characterization. The experimental setup for the analysis is presented in Figure 1, while Figure 2 presents the photographs of the radiographs.

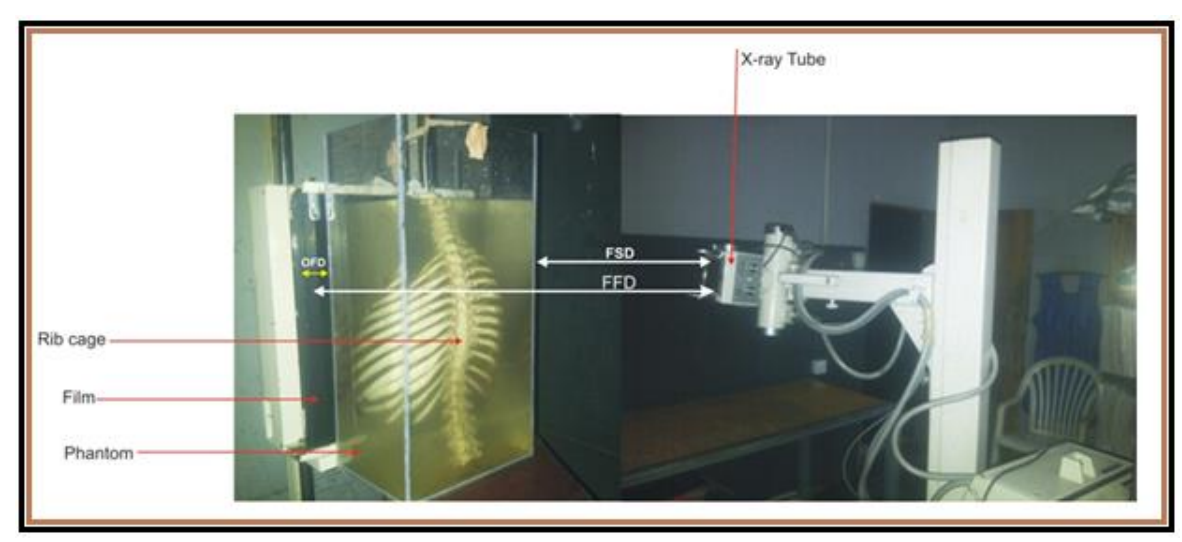


Figure 1: The experimental set-up

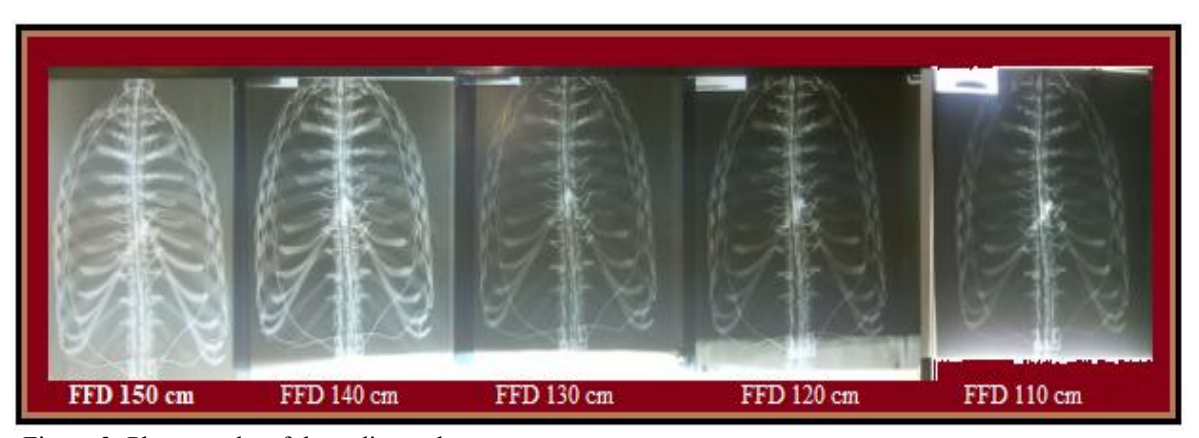


Figure 2: Photographs of the radiographs

#### **Measurement of the Entrance Skin Dose**

The absorbed dose was measured using a RaySafe ThinX dosemeter presented in Figure 3, which was placed at the centre point on the entrance surface corresponding with

the central ray on the phantom and exposed to X-rays with a constant setting of 70 kVp and 10 mAs. The FFD was set at 110, 120, 130,140 and 150 cm for subsequent measurements.

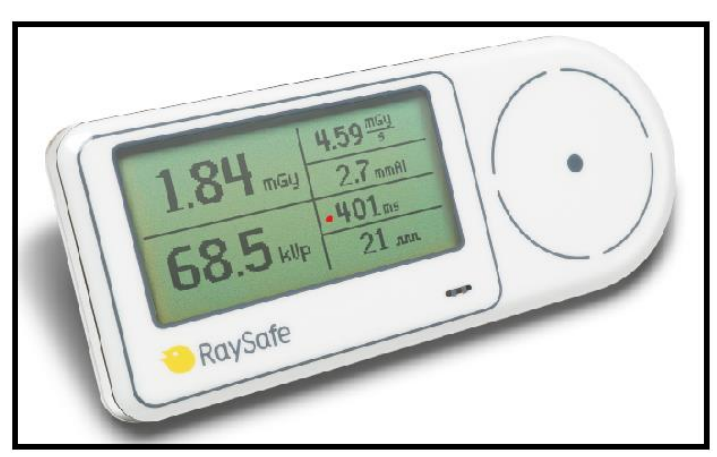


Figure 3: RaySafe ThinX Dosemeter

#### **Determining the Optical Density of the Radiographs**

Figure 4 presents an X-rite 331 transmission densitometer, which was used to measure the optical density of the radiographs. Even though the X-rite 331 transmission densitometer is portable and compact, it has the same accuracy and repeatability as larger countertop

units, measuring densities up to 4.0D and is easy to use. The built-in light table eliminates the need for an external light source and easily accommodates film up to eleven inches wide. The optical density measurement was done at the parts of anatomical interest and the positions of those organs within the thoracic cage.



Figure 4: X-Rite 331 Portable Transmission Densitometer

#### Parts of Anatomical Interest

The optical density for the spaces between the ribs was measured between the  $5^{th}$  and  $6^{th}$  ribs. For the vertebral bodies, it was measured at T12 (thoracic vertebra number 12), which is the last thoracic vertebra. For the lung field's position, the optical density was measured between the  $3^{rd}$  and  $4^{th}$  ribs.

#### Organs within the Thoracic Cage

For the Heart position on the radiographs, the optical density was measured between the  $5^{th}$  and  $6^{th}$  ribs. For the liver, the optical density was measured between the  $7^{th}$  and  $8^{th}$  ribs. For the spleen, the measurement was taken between the  $9^{th}$  and the  $10^{th}$  ribs. Finally, for the kidneys, the optical density was measured between the  $11^{th}$  and the  $12^{th}$  ribs.

## **Image Quality Assessment**

The image quality assessment was based on the European Guideline on Diagnostic Image Quality Criteria for Analytical Criteria (CEC guidelines, 1996). Two Consultant Radiologists and one Radiographer from the Department of Radiology, Jos University Teaching Hospital (JUTH), Jos, Nigeria, Bingham University Teaching Hospital (BUTH), Jos, Nigeria, and University of Jos Health Centre, respectively, scored the anatomical criteria. Visually sharp reproduction of the spaces between the ribs (intercostal space), spinal column, pedicles, vertebral bodies (joints), and lung fields was used as a criterion.

A radiograph demonstrating perfect visualisation was used as a reference image. All images were examined using a constant illuminator and ambient light conditions throughout the study, time and observer; film distance was unrestricted, and all images were assessed blindly (Pengpan et al., 2022).

# Calculation of the Doses Absorbed by the Thoracic Cage

The absorbed dose was simply obtained through the absorbed dose definition (Fragoso-Negrín et al., 2025). Absorbed dose = input dose – output dose (i.e., differences between the input and output dose)  $A_d = I_d - O_d$ 

Where

 $A_d$  = Absorbed dose  $I_d$  = Input dose  $O_d$  = Output dose

#### RESULTS AND DISCUSSION

### **Assessment of the Three Radiologists**

The radiographs at FFD 110, 120, and 130 cm were darker, according to the assessment of the three radiologists, and this was due to very high exposures, which translated to a lot of penetration of the rib cage images. Because of the limited exposure, the radiograph at FFD 150 cm displayed the best contrast. Experts, on the other hand, believe that the radiograph taken at FFD 140 cm produced the best image quality. This indicated that the film's quality was excellent (low optical density), indicating that all the bones of anatomical relevance were

visible and present, and the areas to locate the organs enclosed in the rib cage were also visible (Seth et al., 2022).

Table 1 shows the dependency of the optical density of the radiographs on the film-focus distance (FFD). The results indicated that the highest optical density values (radiographs with much exposure) were obtained at FFD 110 cm, which is the least of the FFDs and decreased with an increase in distance, with the lowest optical density value obtained at FFD 150 cm. That means that more doses were absorbed by these X-ray films at short distances than at long distances (Seth et al., 2022).

Table 1: Effects of Film-Focus (FFD) Distance on the Optical Density of the Parts of Anatomical Interest

FFD (cm)	Optical Density (D) of the Parts of Anatomical Interest						
	Spaces b/w the ribs	Spinal column	Pedicles	Vertebral bodies	Lung fields		
110	2.41	2.18	2.35	2.14	2.41		
120	2.28	1.81	2.11	1.77	2.25		
130	2.11	1.66	1.79	1.64	2.10		
140	1.64	1.08	1.24	1.07	1.62		
150	1.17	0.67	0.70	0.58	1.20		

Table 2 shows the relationship between the total patientabsorbed dose, Film-Focal Distance (FFD) and the optical densities of the organs within the thoracic cavity. The result showed that higher absorbed doses translate to a higher optical density at short distances and lower absorbed doses translate to a lower optical density at long distances.

Table 2: The Relationship between Film-Focus (FFD) Distance, Absorbed Dose, and the Optical Densities of Organs in the Thoracic Cavity

FFD (cm)	Absorbed Dose (mGy)	Optical Density (D) of the Organs in the Thoracic Cavity				
		Heart	Liver	Spleen	Kidney	
110	0.335	2.42	2.38	2.37	2.38	
120	0.283	2.24	2.27	2.23	2.19	
130	0.270	2.03	2.07	1.98	1.89	
140	0.238	1.59	1.58	1.47	1.40	
150	0.222	1.17	1.09	1.00	0.78	

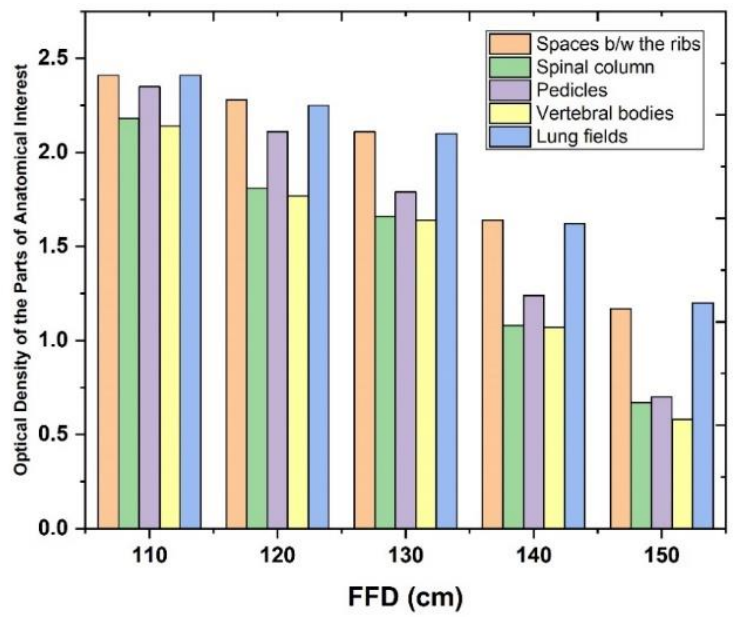


Figure 5: Relationship Between the Optical Density of The Parts of Anatomical Interest and Film-Focus Distance (FFD)

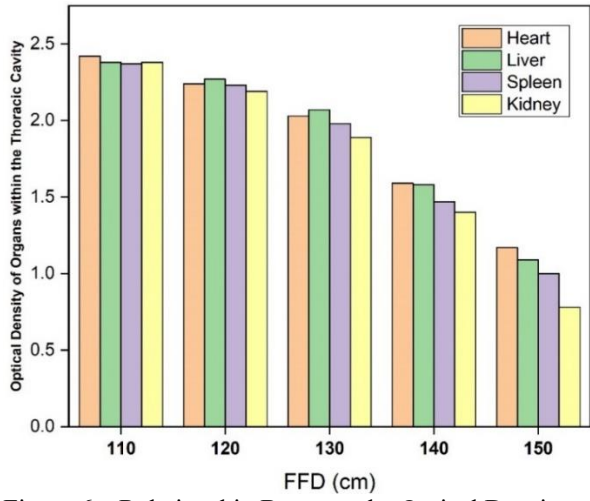


Figure 6a: Relationship Between the Optical Density of Organs Within the Thoracic Cavity and Film-Focus Distance (FFD)

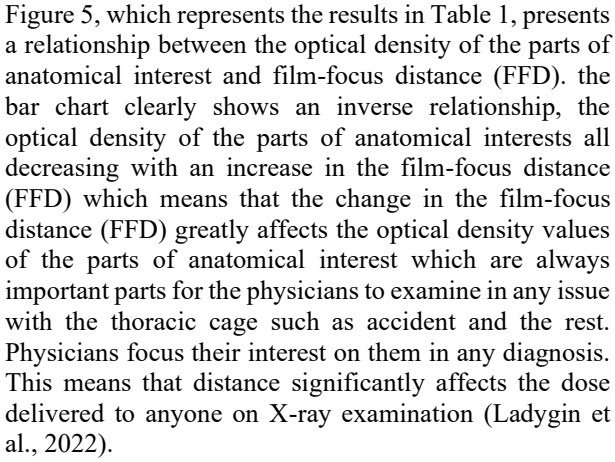


Table 2 and Figure 6 (a) show the relationship between film-focus distance (FFD) and the optical density of the organs within the thoracic cavity. The relationship is also an inverse relationship, which shows a decrease in the optical densities of the organs within the thoracic cage with an increase in film-focus distance (FFD) (Estevan et al., 2010). The optical density of these parts is also very significant for physicians in diagnosis because most of the diseases of these organs are deadly. Diseases such as neonatal lung disorders, acute heart failure, Pneumonia, and COVID-19 virus. Therefore, the clarity of the radiographs to visualise these organs means a lot to physicians.

Table 2 also shows the relationship between film-focus distance (FFD) and absorbed dose. The doses received by these organs also matter a lot to the well-being of an individual. The doses received are not supposed to exceed the permissible dose as recommended by the radiation protection bodies. From Table 2 and Figure 6 (b), the absorbed doses decreased with a decrease in the optical density values of the organs within the thoracic

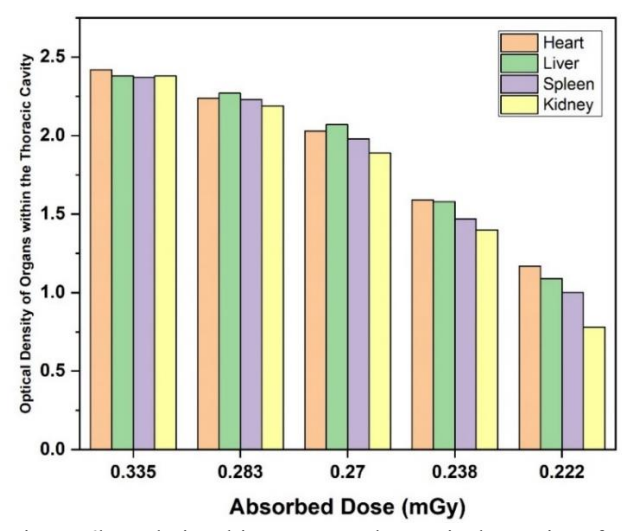


Figure 6b: Relationship Between the Optical Density of Organs Within the Thoracic Cavity and Absorbed Dose

cage, which is a direct relationship. This shows that distance has a tremendous effect on the doses delivered to anyone on X-ray examination, which has its proof in the radiation protection principles such as time, distance and shielding (GIMBA et al., 2021)(Yosua et al., 2024). Just as the heat from a fire reduces as you move further away, the dose of radiation decreases dramatically as you increase your distance from the source.

The absorbed dose of the best radiograph (FFD 140 cm), which is 0.238 mGy, was compared with the standard value (0.300 mGy) given by the radiation management bodies (UNSCEAR, 2000)(Annex & Radiation, 2000)(ICRP, 1991)(Occupational & Procedures, 1996). It was found that the absorbed dose of FFD 140 cm was lower than the standard value, which confirms the validity of the result in this study.

#### **CONCLUSION**

The study reveals that the radiographs of FFD 110, 120, and 130 cm appeared darker, meaning they have high optical density, and this was because of very high exposures, which translated to many doses on the thoracic cage. While the radiograph at FFD 150 cm had the best contrast, this is due to low exposure. However, the best radiograph according to them (experts) is that of FFD 140 cm, which showed clearly all the bones of anatomical interest and the locations of the organs within the thoracic cage. The absorbed dose of FFD 140 cm is 0.238 mGy, which is lower than the standard value (0.300 mGy) given by the global radiation management bodies. This shows that the result is valid since the absorbed dose for the FFD 140 cm is lower than the standard value. This means that lesser doses will be delivered to patients with good image quality if 140 cm FFD is maintained, the voltage to 70 kVp, and the tube load to 10 mAs.

#### REFERENCES

Annex, D., & Radiation, U. N. S. C. on the E. of A. (2000). Sources and effects of ionising radiation. *Investigation of I*, *125*.

Brennan, P. C., McDonnell, S., & O'Leary, D. (2004). Increasing film-focus distance (FFD) reduces radiation dose for X-ray examinations. *Radiation Protection Dosimetry*, 108(3), 263–268.

Bushberg, J. T., & Boone, J. M. (2011). *The essential physics of medical imaging*. Lippincott Williams & Wilkins.

Bushberg, J. T., Seibert, J. A., Leidholdt, E. M., Boone, J. M., & Frank, L. R. (1994). *The essential physics of medical imaging*. Williams & Wilkins, Baltimore.

Curry, T. S., Dowdey, J. E., & Murry, R. C. (1990). *Christensen's physics of diagnostic radiology*. Lippincott Williams & Wilkins.

Daffner, R. H., & Hartman, M. (2013). *Clinical radiology: the essentials*. Lippincott Williams & Wilkins.

Estevan, M., Cotelo, E., Hortal, M., & Iraola, I. (2010). Chest x-ray quality in the diagnosis of pneumonia in children: From prescription to optimization. *Proceedings of IRPA12: 12. Congress of the International Radiation Protection Association: Strengthening Radiation Protection Worldwide-Highlights, Global Perspective and Future Trends*, 10.

Fragoso-Negrín, J. A., Santoro, L., Hébert, K., Kafrouni, M., Vauclin, S., Kotzki, P. O., Pouget, J. P., Deshayes, E., & Bardiès, M. (2025). Methodology for comparing absorbed dose rate calculation algorithms in molecular radiotherapy dosimetry. *Physica Medica*, *133*(March).

GIMBA, Z. A., Sirisena, U. A. I., Chagok, N. M. D., SUNDAY, A. O., ISHAYA, S. D., SETH, E. N., & BONAT, P. Z. (2021). Determination of Optimum Exposure Factors at Constant Focal Film Distance (FFD) to Produce Quality Skull Radiographs with Minimum Absorbed Dose Using a Skull Phantom.

ICRP, I. (1991). publication 60: 1990 recommendations of the International Commission on Radiological Protection. *Ann ICRP*, 21(1–3), 2053748.

Idris, I., & Abdul Manaf, M. R. (2012). Chest X-ray as an essential part of routine medical examination: Is it necessary. *Med J Malaysia*, 67(6), 606–609.

Jain, R., Nagrath, P., Kataria, G., Kaushik, V. S., & Hemanth, D. J. (2020). Pneumonia detection in chest X-

ray images using convolutional neural networks and transfer learning. *Measurement*, 165, 108046.

Khan, R. S., Skapinakis, P., Ahmed, K., Stefanou, D. C., Ashrafian, H., Darzi, A., & Athanasiou, T. (2012). The association between preoperative pain catastrophizing and postoperative pain intensity in cardiac surgery patients. *Pain Medicine*, *13*(6), 820–827.

Ladygin, K. V, Yashina, I. N., Ivanov, A. V, Klochkova, S. V, Nikityuk, D. B., Vodopyanov, O. A., Ladygina, A. I., & Yashin, F. D. (2022). CHANGES IN THE OPTICAL DENSITY OF THE FIRST RIB IN WOMEN DEPENDING ON THE SHAPE OF CHEST AND AGE. Медицинский Вестник Башкортостана, 62.

Liu, J., Lovrenski, J., Ye Hlaing, A., & Kurepa, D. (2021). Neonatal lung diseases: lung ultrasound or chest x-ray. *The Journal of Maternal-Fetal & Neonatal Medicine*, *34*(7), 1177–1182.

Miles, D. A. (2009). Radiographic imaging for the dental team. (*No Title*).

Mousavi, Z., Shahini, N., Sheykhivand, S., Mojtahedi, S., & Arshadi, A. (2022). COVID-19 detection using chest X-ray images based on a developed deep neural network. *SLAS Technology*, *27*(1), 63–75.

Nakao, S., Vaillancourt, C., Taljaard, M., Nemnom, M.-J., Woo, M. Y., & Stiell, I. G. (2021). Diagnostic accuracy of lung point-of-care ultrasonography for acute heart failure compared with chest X-ray study among dyspneic older patients in the emergency department. *The Journal of Emergency Medicine*, 61(2), 161–168.

Occupational, M. S. C. 77 on G. on, & Procedures, P. E. R. from D. N. M. (1996). Sources and magnitude of occupational and public exposures from nuclear medicine procedures.

Pengpan, T., Rattanarungruangchai, N., Dechjaithat, J., Panthim, P., Siricharuwong, P., & Prapan, A. (2022). Optimisation of Image Quality and Organ Absorbed Dose for Pediatric Chest X-Ray Examination: In-House Developed Chest Phantom Study. *Radiology Research and Practice*, 2022, 1–10.

Peters, S. E., & Brennan, P. C. (2002). Digital radiography: are the manufacturers' settings too high? Optimisation of the Kodak digital radiography system with aid of the computed radiography dose index. *European Radiology*, 12(9), 2381–2387.

Schaefer-Prokop, C., Neitzel, U., Venema, H. W., Uffmann, M., & Prokop, M. (2008). Digital chest

radiography: an update on modern technology, dose containment and control of image quality. *European Radiology*, *18*, 1818–1830.

Seth, N., Corresponding, E., Sirisena, U. A. I., & Seth, J. (2022). INTERNATIONAL JOURNAL OF SCIENTIFIC RESEARCH THE USE OF THE EXTENDED FILM-FOCUS DISTANCE TECHNIQUE FOR DOSE REDUCTION: EXAMINATION OF THE THORACIC (RIB) CAGE Physics Dembo. 2277, 10–12.

UNSCEAR, U. N. (2000). Sources and effects of ionising radiation. *United Nations Scientific Committee on the Effects of Atomic Radiation*.

Valentin, J. (2004). Managing patient dose in digital radiology. *ANNALS-ICRP*, 34(1), 21–49.

Vano, E., Fernández, J. M., Ten, J. I., Prieto, C., Gonzalez, L., Rodriguez, R., & de Las Heras, H. (2007). Transition from screen-film to digital radiography: evolution of patient radiation doses at projection radiography. *Radiology*, 243(2), 461–466.

Veldkamp, W. J. H., Kroft, L. J. M., & Geleijns, J. (2009). Dose and perceived image quality in chest radiography. *European Journal of Radiology*, 72(2), 209–217.

Venema, H. W., van Straten, M., & den Heeten, G. J. (2005). Digital radiography of the chest: reassessment of the high-voltage technique? *Radiology*, *235*(1), 336–338.

Walter, H. (2010). *Review of Radiologic Physics*. Philadelphia Wolters Kluwer Health.

White, S. C., & Pharoah, M. J. (2013). *Oral radiology:* principles and interpretation. Elsevier Health Sciences.

Yosua, I. N., Sutapa, G. N., Putra, I. K., Suryatika, I. B., Suyanto, H., & Paramarta, I. B. A. (2024). The Effect of Focus Film Distance Variation on Patient Absorbed Dose in Thorax Examination with Roentgen Machine in Radiology Installation of Sanjiwani Hospital Gianyar. *Kappa Journal*, 8(3), 446–450.